Spectral hole burning quantum efficiency and electron traps in Sm^{2+}-ion-doped aluminosilicate glasses

Hongwei Song, Tomokatsu Hayakawa, and Masayuki Nogami*
Nagoya Institute of Technology, Showa Nagoya, 466-8555, Japan
(Received 12 November 1998)

Persistent spectral hole burning (PSHB) in the $^7F_0$-$^5D_0$ transition and the electron excitation in the $^7F_0$-$4f5d$ transition of Sm^{2+} doped in Al_2O_3-SiO_2 glasses were studied from the measurements of hole burning efficiency and the refilling of the burnt hole. The PSHB at low temperature is attributed to the optically activated rearrangement of OH bonds surrounding Sm^{2+} ions. On the other hand, the PSHB at high temperature is attributed to one-step electron tunneling in the excitation state. The barrier heights for hole filling corresponding to the two mechanisms were determined to be ~0.27 and ~0.90 eV, respectively. Thermal depth of the trap that captures electrons by two-step ionization via the $4f5d$ state was determined to be ~0.35 eV below the conduction band. A model was proposed for describing the PSHB and electron excitation of Sm^{2+} doped in Al_2O_3-SiO_2 glasses. In addition, the dependence of hole burning efficiency on the Al_2O_3 concentration, temperature, and burning wavelength was also studied. [S0163-1829(99)05917-2]

I. INTRODUCTION

Since the first observation of photon-gated persistent spectral hole burning (PSHB) phenomenon in BaFCl:Sm^{2+} crystal was reported by Winnaker, Shelby, and Macfarlane in 1985,[1] many studies have been carried out to develop the Sm^{2+}-doped PSHB material because of its potential use in high-density frequency-domain optical storage. For practical use, high-temperature PSHB is required. In a Sm^{2+}-doped $BaFCl_{0.5}Br_{0.5}$ mixed crystal, PSHB at liquid-nitrogen temperature was observed for the first time by Yu and coworkers in 1989.[2] Then, further room-temperature PSHB was also observed in the Sm^{2+}-doped $M_yM'_{1-y}FCl_xBr_{1-x}$ (M and M' = Mg, Ca, Sr, and Ba) mixed crystals.[3–6] The observation of PSHB at room temperature is significant for the development of new optical memory devices. Recently, room-temperature PSHB was also observed in Sm^{2+}- and Eu^{3+}-doped glasses.[7–10] As a host material, glasses are thought to be more favorable than crystals or mixed crystals because of their wide inhomogeneous linewidth, compositional variety, and easy mass production.[11] In the Sm^{2+}-doped glasses, since the silicate glasses surpass fluoride and borate glasses in chemical durability, it thus becomes possible to move beyond the limitations of these fluoride and borate glasses.[12]

In the past, some characteristics of Sm^{2+}-doped alminosilicate glasses prepared by a sol-gel method such as fluorescence, high-temperature PSHB, and electron excitation process were revealed to some extent.[9,12–14] Despite this, it is still worthwhile to make further investigation into some aspects. On the one hand, the PSHB mechanism of Sm^{2+} in the host of alminosilicate glasses as well as in the other glasses is not clarified. The question where the electrons produced by the ionization of Sm^{2+} are captured still remains unknown. On the other hand, the hole burning quantum efficiency in Sm^{2+}-doped glasses is too low for optical memory. For practical use, it should be greatly enhanced. Therefore, the search for hole burning in Sm^{2+}-doped glasses is necessary for both the understanding of the mechanism of hole burning and the development of new materials with the development of the properties required for optical memory devices at present.

In this paper, we mainly report our studies on the electron traps and hole burning quantum efficiency in the Sm^{2+}-doped Al_2O_3-SiO_2 glasses. Surrounding the hole burning quantum efficiency, we measured and compared the hole burning processes in the Al_2O_3-SiO_2 glasses with a different concentration of Al_2O_3 at room temperature. The dependence of PSHB quantum efficiency on the glass temperature and burning wavelength was also studied. To reveal the PSHB mechanism and electron traps, the temperature-cycling experiment of a burned hole was performed in a Sm^{2+}-doped $15Al_2O_3 \cdot 85SiO_2$ glass from 8 or 200 K, respectively. The thermal depth of one trap that captures electrons through the conduction band was determined by the spectra change upon irradiation of laser with energy corresponding to the f-d transition of the Sm^{2+} ions. Origins of the electron traps for the PSHB and electron excitation were analyzed.

II. EXPERIMENTS

The Sm^{3+}-containing aluminosilicate glasses were prepared by the sol-gel method. The glass compositions are, respectively, $15Al_2O_3 \cdot 85SiO_2$, $10Al_2O_3 \cdot 90SiO_2$, $5Al_2O_3 \cdot 95SiO_2$, and $2Al_2O_3 \cdot 98SiO_2$ (mol %) containing normally 5 wt % Sm_2O_3. To reduce the Sm^{3+} ions to Sm^{2+}, the glasses were heated at 800 °C under flowing H_2 gas. A detailed explanation of the glass preparation is given elsewhere.[13,14]

A hole was burned in the $^7F_0$-$^5D_0$ line by a pulsed Nd:YAG (yttrium-aluminum-garnet) laser-pumped dicyanoimidazole (DCM) dye laser with a repetition frequency of 10 Hz and a bandwidth of ~0.8 Å full width at half maximum. The excitation spectra before and after hole burning were recorded by scanning the laser from 683.0 to 687.0 nm while monitoring the fluorescence of the $^5D_0$-$^7F_2$ transition at 726.0 nm. The laser power for reading the holes was at-

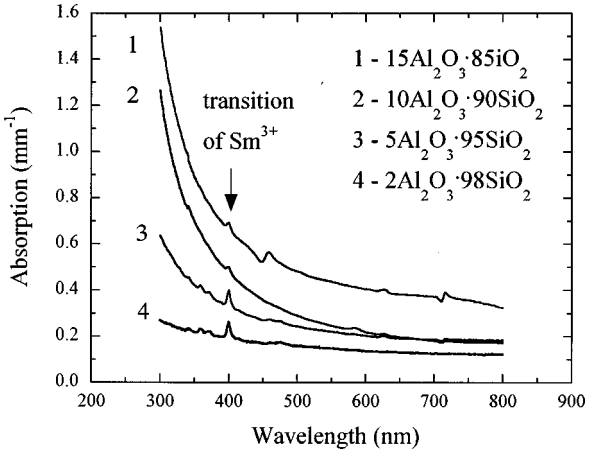

FIG. 1. Absorption spectra of Sm-doped Al_2O_3-SiO_2 glasses measured at room temperature.

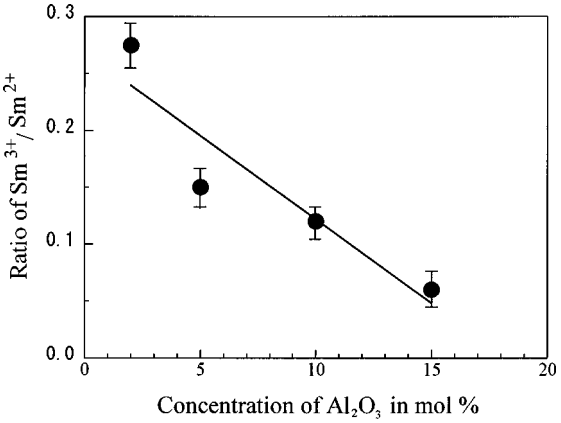

FIG. 2. The ratio of the absorption coefficient contributed by the f-f transition of Sm^{3+}, to that contributed by the f-d transition of Sm^{2+} versus Al_2O_3 concentration.

tenuated by neutral-density (ND) filters to be less than 0.1% of that for burning. In the temperature-cycling experiments of the hole spectra, the sample was contained within a helium gas closed-cycling cryostat. A hole was burned at 8 or 200 K, respectively. After cycling through a certain temperature higher than the burning temperature and maintaining for 300 s, the residue hole was again measured at 8 or 200 K. A continuous argon-ion laser with whole lines was used to irradiate the sample with the energy corresponding to the f-d transition of Sm^{2+}. The optical-absorption spectra were measured with a spectrometer.

III. RESULTS

A. Absorption spectra of Sm-doped Al_2O_3-SiO_2 glasses

Figure 1 shows the absorption spectra in the range of 300–800 nm in the Sm-doped Al_2O_3-SiO_2 glasses. The band-shaped absorption in the range of 300–800 nm is attributed to the f-d transition ($^7F_0$-$^5D_0$) of Sm^{2+}. The sharp absorption peak at 406 nm is attributed to one of the f-f transition ($^6H_{5/2}$-$^6P_{3/2}$) of Sm^{3+}. According to Fig. 1, the ratio of the absorption coefficient contributed by Sm^{3+} and that contributed by Sm^{2+} at 406 nm is determined. This value should be proportional to the ratio of the density of Sm^{3+} to that of Sm^{2+}. Figure 2 shows the ratio of Sm^{3+}/Sm^{2+} as a function of Al_2O_3 concentration. As shown in Fig. 2, the ratio of Sm^{3+}/Sm^{2+} decreases with the increase of Al_2O_3 concentration. We should point out that the ratio of Sm^{3+}/Sm^{2+} obtained is not an absolute value but a relative one.

B. Spectral hole burning of Sm^{2+}-doped Al_2O_3-SiO_2 glasses

At room temperature, a hole was burned with a fixed laser power density at 500 mW/cm^2 for 20 min in the Sm^{2+}-doped glasses. The excitation intensity at the burned site (685 nm) was monitored as a function of burning time and before and after hole burning. Figure 3 shows typical excitation spectra of the $^7F_0$-$^5D_0$ transition before and after hole burning and their differential spectra for glasses with different concentration of Al_2O_3. It is observed that the position of excitation spectra shifts to the short wavelength side with the increase of the Al_2O_3 concentration. After burning for 20 min, a hole is formed in all the glasses, and the hole depth and hole width vary with the Al_2O_3 concentration. In the $15Al_2O_3{\cdot}85SiO_2$ glass, a hole with a depth of ~18% and a width of ~2.4 nm is formed. In the other glasses, the hole depth is shallower and the hole width is narrower. The dependence of the hole depth at 685 nm on the burning time was measured as a change in the excitation intensity while monitoring the fluorescence at 726 nm, which is shown in Fig. 4. It is evident that the hole burning dynamics are well fitted with exponential functions in the $15Al_2O_3{\cdot}85SiO_2$ and $5Al_2O_3{\cdot}95SiO_2$ glasses. In the other glasses, a hole is also formed exponentially. This exponential dynamics definitely reveals that it is one main trap that captures the ionized elec-

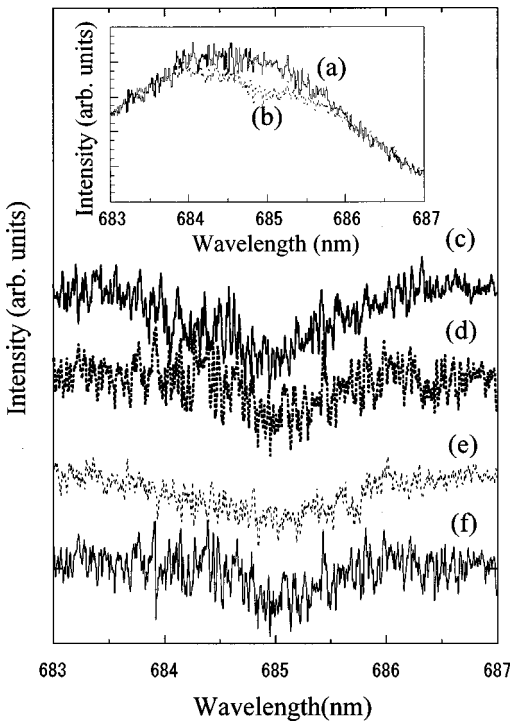

FIG. 3. Difference between the excitation spectra before and after hole burning for glasses with different concentration of Al_2O_3 at room temperature. (c), $15Al_2O_3{\cdot}85SiO_2$; (d), $10Al_2O_3{\cdot}85SiO_2$; (e), $5Al_2O_3{\cdot}95SiO_2$: (f), $2Al_2O_3{\cdot}98SiO_2$. Inset: A typical excitation spectrum of the $^7F_0$-$^5D_0$ transition before (a), and after (b) hole burning in the $15Al_2O_3{\cdot}85SiO_2$ glass.

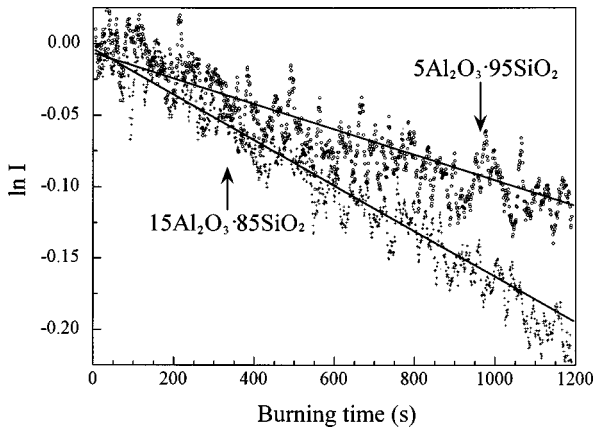

FIG. 4. Logarithm of the normalized excitation intensity: I at the burned site (685.0 nm) as a function of burning time corresponding to the PSHB experiments in Fig. 3.

trons at room temperature. In Fig. 4, the hole burning rate R_H can be estimated from the hole burning dynamics according to Eqs. (5) and (8). R_H is proportional to hole burning quantum efficiency and hence is an important parameter for PSHB.[15] Figure 5 shows the dependence of R_H and the hole depth on the concentration of Al_2O_3. It is evident that hole depth and the burning rate both increase with the increase of Al_2O_3 concentration.

While a hole is formed by the optical irradiation of the burning light, a part of the hole is also thermally and optically filled in the same time. And, the lifetime of the excited state, which has an effect on the PSHB, depends on temperature. Therefore, the hole burning rate and hole burning quantum efficiency depend on temperature. At different temperatures, a hole was burned with a fixed laser density of 125 mW/mm^2 for 600 s at 686.5 nm for the $15Al_2O_3{\cdot}85SiO_2$ glass. The excitation intensity at the burning site was recorded as a function of time and temperature. The burning rate and hole depth after burning for 600 s are plotted in Fig. 6 as a function of temperature. It is evident that both the R_H and the hole depth decrease with increasing temperature. The experimental data of R_H were fitted with a linear function of temperature T as follows:

$$R_H=(7.02-0.022\times T)\ \ 10^{-5}\ \ \mathrm{s}^{-1}. \tag{1}$$

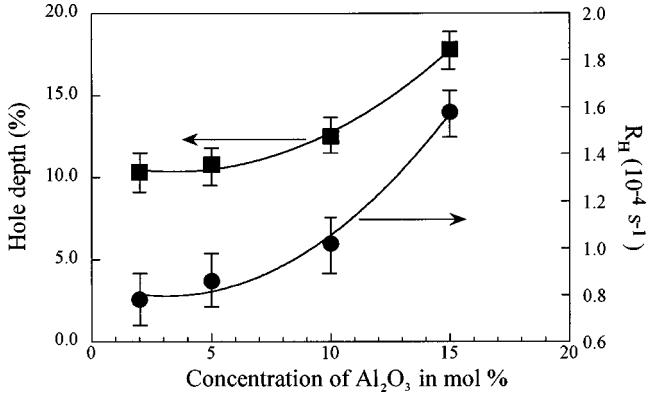

FIG. 5. Hole burning rate R_H and the hole depth after burning for 20 min versus the Al_2O_3 concentration in Sm^{2+}-doped Al_2O_3-SiO_2 glasses. The laser density was fixed at 500 mW/mm^2.

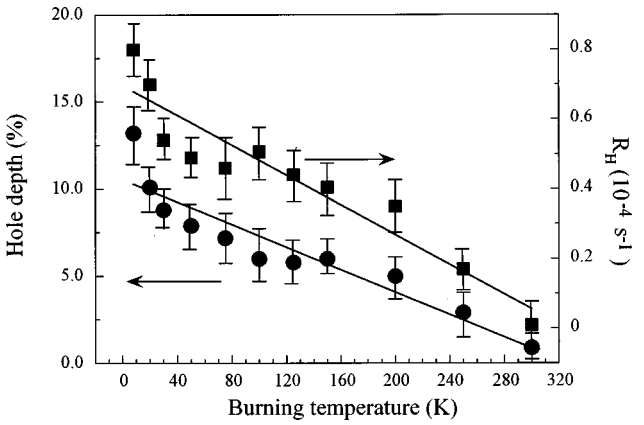

FIG. 6. Hole burning rate R_H and hole depth after burning for 10 min as a function of temperature. The laser density of the burning light was fixed at 125 mW/mm^2 and the burning site is at 686.5 nm.

At 8 K, R_H is in the order of $10^{-4}\,\mathrm{s}^{-1}$ and at 300 K is only in the order of $10^{-6}\,\mathrm{s}^{-1}$. In some hole burning materials, it has been found that the hole burning quantum efficiency depends strongly on burning wavelength.[16] One of the reasons may be that the electron transition probability is different at different sites within an inhomogeneous line.[16,17] At 80 K, a hole was burned at different sites of the $^7F_0$-$^5D_0$ line with a fixed laser density at 125 mW/mm^2 for 600 s. Figure 7 shows the relation between the hole depth and hole burning wavelength. It is evident that both the hole depth and the hole burning rate are independent of the wavelength within the error of 10%.

To study the stability of the burnt hole near room temperature, the hole that was burned at 250 and 300 K was measured in the dark at that temperature. The normalized hole area is plotted in Fig. 8 as a function of time. The solid dots and the solid lines are, respectively, the experimental data and the fitting functions based on a Gaussian distribution. Theoretically, the fraction of the remaining hole can be given as

$$F(t)=1-\int_{-\infty}^{+\infty} g(V)\exp(-Rt)\,dV. \tag{2}$$

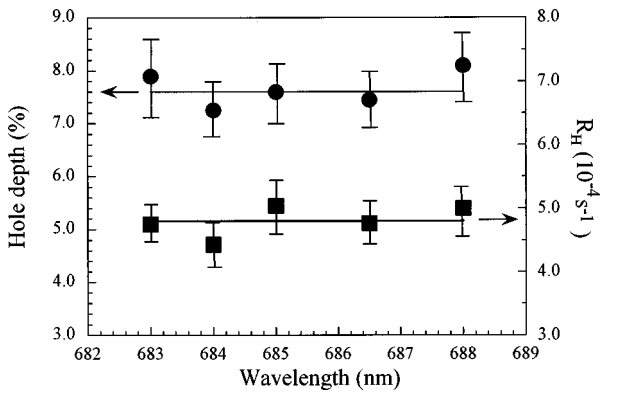

FIG. 7. Hole burning rate R_H and hole depth after burning for 10 min as a function burning wavelength measured at 80 K. The laser density of burning light was fixed at 125 mW/mm^2.

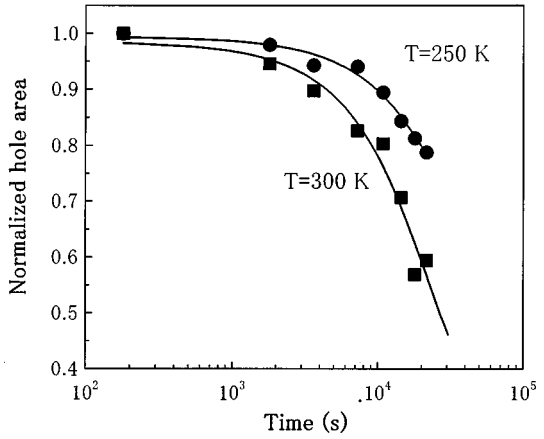

FIG. 8. Normalized hole area as a function of time in the dark at 250 and 300 K. The solid dots are experimental data and the solid lines are fitting functions based on Gaussian distributions.

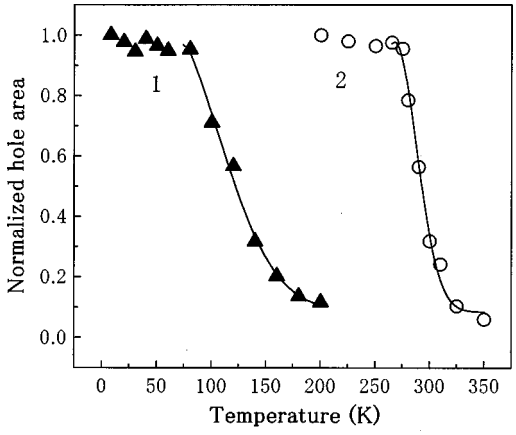

FIG. 9. Normalized hole area as a function of the cycling temperature. A hole was burned and detected, respectively, at 8 and 200 K. Solid curves indicate fits to data based on Gaussian distribution functions.

Generally, $g(V)$ is taken as a Gaussian distribution function. While a barrier is wide, $F(t)$ decays approximately with a Gaussian function. While a barrier is narrow, $F(t)$ decays approximately with an exponential function. At 300 K, the lifetime (e^{-1}) of the burned hole is determined to be $\sim 3.2\times 10^4$ s. This value is smaller than that in the Sm^{2+}-doped single crystal.[5]

C. Thermal refilling behavior of the burnt hole

The hole burnt state has a higher energy than the unburned state and it relaxes across the activation barrier into the unburned state. The stability of the hole burnt state can be discussed from the temperature-dependent and time-dependent hole erasure experiments. In this reaction, the optically activated state relaxes across the activation barrier V into the unburned state, the rate of which is given as

$$R = R_0 \exp(V/kT), \tag{3}$$

where R_0 is the attempt frequency, k is the Boltzmann constant, and T is the temperature in K. Assuming that the barrier height follows a Gaussian distribution and the fraction of the remaining hole F is proportional to the number of photo products of the burnt state that remain unchanged. The fraction of the remaining hole is presented as a function of the holding temperature higher than the burning temperature,

$$F(T) = 1 - \int_0^{kT\ln(R_0 t_0)} g(v)dV, \tag{4}$$

where t_0 is the holding time at temperature T. Figure 9 shows the hole area as a function of the cycling temperature, where the hole area is normalized to unity at the burning temperature of 8 and 200 K. The area of the hole burned at 8 K decreases slowly with increasing temperature up to 80 K and decreases rapidly above 80 K. On the other hand, the area of the hole burned at 200 K decreases rapidly in the range of 270–350 K. Both of the obtained data are well fitted with Gaussian distribution functions; the constant parameters of the barrier height and the width are obtained as $V_1 = 0.27 \pm 0.05$ eV and $\delta_1 = 0.08 \pm 0.02$ eV for the hole burned at 8 K and $V_2 = 0.90 \pm 0.10$ eV and $\delta_2 = 0.05 \pm 0.02$ eV for the hole burned at 200 K, respectively, using the fitting parameters of $R_0 = 10^{14}$ s^{-1} and $t_0 = 300$ s.

D. Two-step excitation via the $4f5d$ state

According to Ref. 12, on the excitation of laser light corresponding to the $4f5d$ excitation, the fluorescence intensity of $^5D_0$-^7F_J decreases significantly at 77 K, accompanied by the production of optical current. This means that some electrons excited to the $4f5d$ bands from the ground state of Sm^{2+} are excited to the conduction band further by the second photons. At 8 K, we measured the excitation intensity on the optical irradiation with an argon-ion laser. Figure 10 shows the excitation spectra of the $^7F_0$-$^5D_0$ transition on the optical irradiation with the argon laser while the laser power is changed. It is evident that the excitation intensity decreases significantly on the optical irradiation. Figure 11 shows the dependence of the intensity of the $^7F_0$-$^5D_0$ transition on the laser power of the irradiation light. It is evident that the excitation intensity decreases rapidly with increasing the argon-ion laser to almost become zero at 50 mW. The reversible responses were also observed while the argon laser

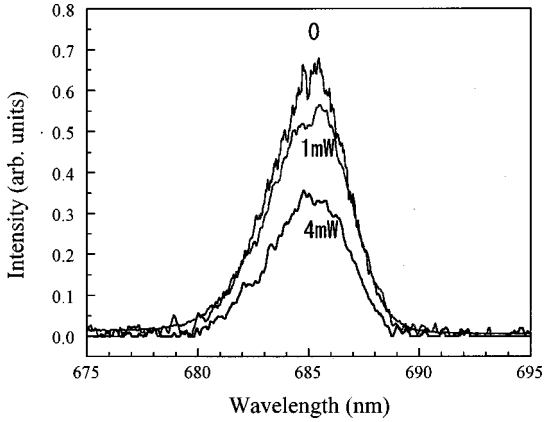

FIG. 10. Excitation spectra of the $^5D_0$-$^7F_0$ transition on the optical irradiation with an argon-ion laser while the power was changed. The spectra were measured by monitoring the $^5D_0$-$^7F_2$ emission at 726 nm.

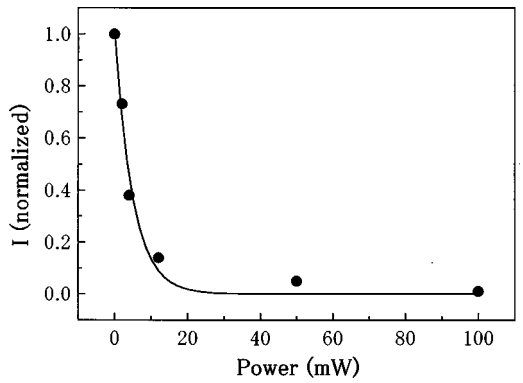

FIG. 11. The excitation intensity of the $^5D_0$-$^7F_0$ transition versus the power of the argon-ion laser.

was turned on and turned off. It was found that the excitation intensity changes with a fast response shorter than 100 ms. Therefore, the temporal decrease of the excitation intensity is mainly attributed to the complete optical excitation between the $^7F_0$-$^5D_0$ transition and the $^7F_0$-$4f5d$ one. After the optical irradiation with a power of 100 mW for more than 20 min, the argon-ion laser was turned off. The excitation spectrum was measured again and compared with that before the optical irradiation. After irradiation, the intensity of $^7F_0$-$^5D_0$ has a decrease of ~5%. The permanent decrease of the intensity of $^7F_0$-$^5D_0$ is attributed to the electrons in the conduction band captured by one certain trap.

When the temperature is elevated, some of electrons within the traps will thermally relax and recombine with the ionized Sm^{2+} (Sm^{3+}). Accordingly, the excitation intensity of the $^7F_0$-$^5D_0$ transition increases while it is measured at 8 K again. Figure 12 shows a normalized intensity, which is proportional to the number of residue electrons in the traps, versus the cycling temperature. The thermal depth V_3 and the width δ_3 of the electron trap were determined by fitting the experimental data with a Gaussian distribution function to be ~0.35 and ~0.17 eV, respectively.

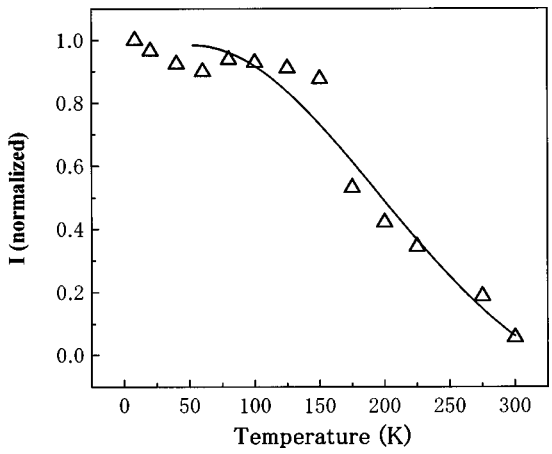

FIG. 12. Normalized intensity I versus the cycling temperature. Here, $I=[I_B-I_A(T)]/(I_B-I_A)$, I_B and I_A present the $^5D_0$-$^7F_0$ excitation intensity before and after optical irradiation at 8 K, respectively, I_A (T) presents the intensity measured at 8 K after cycling to T and maintaining for 300 s. I is proportional to the number of residue electrons within the traps.

IV. DISCUSSIONS

A. Hole burning mechanism and electron traps

In the Sm^{2+}-doped crystals, a hole is usually formed by photon-gated PSHB and the main electron trap is considered to be Sm^{3+}.[1] On the other hand, in the Sm^{2+}-doped fluoride and borate glasses, a hole is usually formed by a one-step excitation and the main electron trap is considered not to be Sm^{3+}.[7,18] Recently Nogami and co-workers found that the Eu^{3+}-doped glasses prepared by the sol-gel method show the PSHB at a high temperature, such as 200 K, and the hole depth linearly increases with increasing the OH content.[11,19] The proposed model for hole burning in these glasses is that the hole is burned by the optically activated rearrangement of the OH bonds surrounding the Eu^{3+} ions.[11,19] The barrier height V for hole filling was estimated to be ~0.31 eV for the Eu^{3+}-doped Al_2O_3-SiO_2 glasses, which is considered to correspond to the energy necessary for the rearrangement of OH bonds surrounding the Eu^{3+} ions.[19] Since the Sm^{2+}-doped glasses prepared in this study also contain OH bonds, the hole burning can occur due to the rearrangement of the OH bonds.[20] The glasses used in the present study are heated at 800 °C in preparation. OH bonds still exist at that temperature.[20] Therefore, we can attribute the formation of PSHB of Sm^{2+} at low temperature to the optically activated rearrangement of the OH bonds surrounding the Sm^{2+} ions. The determined value of V_1 (~0.27 eV) is also in agreement with the barrier height for hole filling caused by the rearrangement of OH bonds (~0.31 eV) obtained for the Eu^{3+} ion-doped glasses.

In the hole burning at 200 K, the barrier height V_2 for hole refilling is ~0.90 eV. The hole burning of Sm^{2+} at high temperature could be attributed to the one-step electron tunneling in the excited state because the hole area was observed to be proportional to the laser density of burning light instead of the square of the laser density.[12] According to the results shown in Fig. 2, the ratio of Sm^{3+}/Sm^{2+} decreases with increasing the Al_2O_3 concentration, meaning that the density of the electron trap surrounding Sm^{2+} should decrease with increasing the Al_2O_3 concentration if Sm^{3+} ions act as electron traps at high temperature. Accordingly, the hole burning quantum efficiency should decrease with increasing the Al_2O_3 concentration. The reverse result of hole burning at room temperature (see Figs. 3–5) excludes the possibility of Sm^{3+} ions acting as electron traps. We should also point out that no antihole was observed in the two sides of the burned hole, which also shows that Sm^{3+} ions are not the main traps. On the contrary, the present result for hole burning at room temperature suggests that the electron traps possibly relate to Al ions. In fact, because of weak bonding of Al with oxygen, Al^{2+}, Al^{3+} may both exist in the glass network. It is easy for Al^{3+} to transfer into Al^{2+} when it captures an electron from the excited state of Sm^{2+}. Therefore, we suggest that the increasing density of the Al^{3+} ion, the possible electron trap, is one of the possible reasons for increasing hole burning quantum efficiency with the Al_2O_3 concentration. Co-doping of Al_2O_3 in the silicate glasses was also observed to be favored by the emissions of the Sm ions.[14] Increasing hole burning quantum efficiency with the Al_2O_3 concentration at room temperature also excludes the possibility of Si ions acting as the electron traps. Because of

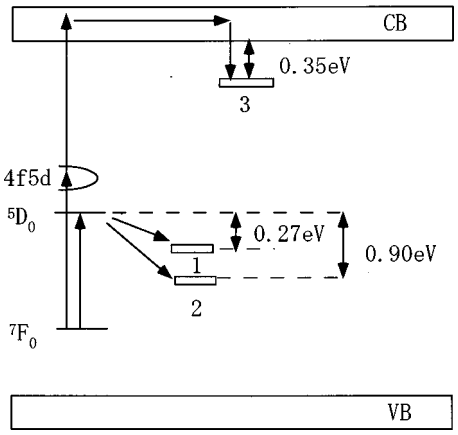

FIG. 13. A model for the explanation of the PSHB and electron excitation of Sm^{2+} in the alminosilicate glasses. Here, the barrier 1 is formed by the optically activated rearrangement of OH bonds surrounding Sm^{2+} and the barrier 2 is formed by the electron tunneling in the excited state.

the strong bonding of the Si with oxygen, it is difficult for Si to exist with the other valence states besides 4+ in the glass network. Generally, the electron trap in hole-burning materials cannot be identified by the method of hole burning itself. Further work should be performed on identifying the electron trap in Al_2O_3-SiO_2 glasses by the other techniques such as the light-induced electron spin resonance spectrum.

The other trap ($V_3=0.35$ eV) that captures the electrons by two-step excitation via $4f5d$ of Sm^{2+} is considered to be independent of the optically activated rearrangement of OH bonds, although its thermal depth is close to 0.31 eV, the barrier height corresponding to the rearrangement of the OH bonds. The reason is that some Sm^{2+} ions have been ionized during the irradiation of an argon laser judged by the production of optical current. Of course, it is a different electron trap compared with the 0.90 eV one. It is attributed to a certain shallow level below the conduction band with a broadened width. At 8 and 300 K, a hole was burned before and after the optical irradiation with an argon laser. The result shows that the hole burning quantum efficiency does not change before and after the irradiation, suggesting that the electron trap capturing the electrons by the two-step excitation is not related to the OH bond. Otherwise, the hole burning efficiency after optical irradiation will decrease because of the previous occupation of the traps before hole burning.

According to the present study, a detailed model for PSHB and electron excitation of Sm^{2+}-doped Al_2O_3-SiO_2 glasses can be drawn, as shown in Fig. 13.

B. Hole burning efficiency

Under the condition of $\mu \leqslant \tau \leqslant T$ (μ is the width of laser pulse, τ is the electron lifetime of the $^5D_0$ level, and T is the interval of laser pulses) an approximate solution can be derived by the dynamical equations of the three-level system for hole burning in the $^7F_0$-$^5D_0$ transition with a pulsed laser. The three levels are the ground state $|0\rangle$ ($^7F_0$), the excited state $|1\rangle$ ($^5D_0$), and the trapping state $|2\rangle$, respectively. The hole depth can be given as

$$D(t)=1-\exp(-at) \tag{5}$$

with

$$a=\ln(1-\beta) \tag{6}$$

and

$$\beta=\frac{R_{10}R_{12}}{R_1}qI, \tag{7}$$

where D is the normalized hole depth, R_{10} is the electron transition rate from $|1\rangle$ to $|0\rangle$, R_{12} is the electron trapping rate from $|1\rangle$ to $|2\rangle$, R_1 is the total electron transition rate of $|1\rangle$, including radiative and nonradiative transition ones, which equals the inverse of the lifetime of $|1\rangle$, q is the ratio of electron transition rate R_{10} to the absorption cross section from $|0\rangle$ to $|1\rangle$, and I is the laser intensity of the burning light. According to Eq. (5), the hole burning rate R_H while t approaches 0 can be written as

$$R_H=\left.\frac{dD}{dt}\right|_{i\to 0}=a. \tag{8}$$

When the laser intensity of the hole burning light is not so strong and $\beta \ll 1$, R_H can be written as

$$R_H \approx \frac{R_{10}R_{12}}{R_1}qI. \tag{9}$$

Here we should point out that the electron trapping is proposed to be a single-molecule process. And, the number of the electron trap is considered to be infinite. Thus, the hole depth can approach 100% according to Eq. (5). The equations above are valid only in the beginning of hole burning. It was observed that the hole burning dynamics at different temperatures are all in accordance with an exponential rule within the burning time of 600 s.

The hole burning rate increases with increasing the Al_2O_3 concentration (see Fig. 5). According to Eq. (9), one possible reason is that the electron transition rate R_{10} and R_1 varies with the Al_2O_3 concentration, and leads to the increase of R_{10}/R_1, as well as R_H, with increasing the Al_2O_3 concentration. In the Sm^{2+}-doped $BaFCl_xBr_{1-x}$ mixed crystals, it was found that R_{10} increases with increasing the Br concentration.[21] The other possible reason, which has been mentioned in Sec. IV A, is that the electron trapping rate R_{12} increases with increasing the Al_2O_3 concentration. R_{12} depends strongly on the density of the electron trap, the Al^{3+} ion. According to Eq. (9), R_H should decrease with temperature because R_1 increases with temperature, as shown in Fig. 6. In Eq. (9), if R_{10} or R_1 changes with wavelength in the inhomogeneous line, R_H will vary with wavelength also. The independent relationship between R_H and wavelength in Fig. 7 shows that R_{10} or R_1 is independent of wavelength in Sm^{2+}-doped Al_2O_3-SiO_2 glasses.

In order to increase the hole burning quantum efficiency, R_{10} and R_{12} should be enhanced. On the contrary, R_1 should be decreased. A better host is expected to make the electron transition probability of $^7F_0$-$^5D_0$ and density of the electron trap both increase greatly.

V. CONCLUSIONS

At room temperature, a hole was burned in Sm^{2+}-doped Al_2O_3-SiO_2 glasses with a different concentration of Al_2O_3 under the same conditions. The results show that the hole burning quantum efficiency increases with increasing the Al_2O_3 concentration. On the other hand, the ratio of Sm^{3+}/Sm^{2+} decreases with increasing the Al_2O_3 concentration, suggesting that the traps that capture electrons ionized from Sm^{2+} are not Sm^{3+}, but may be some other impurity levels, such as Al^{3+}. It is apparent that the hole burning quantum efficiency decreases linearly with increasing temperature and almost independent of burning wavelength.

For the hole burned at 8 and 200 K by the one-step excitation of $^7F_0$-$^5D_0$ transition, the temperature-cycling experiments of the burnt hole were performed. The main mechanism for the hole burning can be concluded to vary with the burning temperature. At low temperature, PSHB is attributed to the rearrangement of OH bonds surrounding Sm^{3+} ions. At high temperature, PSHB is attributed to one-step electron tunneling in the excited state. The barrier heights for hole filling, corresponding to the two mechanisms of PSHB, were determined to be $\sim$0.27 and $\sim$0.90 eV, respectively. On the other hand, the two-step ionization via the $4f5d$ bands, the population of Sm^{2+}, and the excitation intensity of $^7F_0$-$^5D_0$ decrease, correspondingly, the electrons that are captured by the other trap below the conduction band. From the temperature-cycling experiment, the depth of the trap was determined to be $\sim$0.35 eV. The stability of the burned hole was studied near room temperature. The time constant of the burned hole was deduced to be $\sim 3.2\times10^4$ s at 300 K.

In conclusion, we could draw the detailed model for the PSHB and the optical excitation of the Sm^{2+}-doped in Al_2O_3-SiO_2 glasses. We believe that the hole burning mechanism of the Sm^{2+}-ion doped in Al_2O_3-SiO_2 glasses is becoming clearer through our present studies.

ACKNOWLEDGMENTS

This research was partly supported by a Grant-in-Aid for Scientific Research (No. 09650734) from the Ministry of Education, Science, and Culture of Japan.

*Author to whom correspondence should be addressed. FAX: 81 52 735 5285; electronic address: nogami@mse.nitech.ac.jp

[1] A. Winnaker, R. M. Shelby, and R. M. Macfarlane, Opt. Lett. **10**, 350 (1985).
[2] C. Wei, S. Huang, and J. Yu, J. Lumin. **43**, 161 (1989).
[3] J. Zhang, S. Huang, and J. Yu, Chin. J. Lumin. **12**, 181 (1991).
[4] K. Holloday, C. Wei, M. Croci, and Urs. P. Wild, J. Lumin. **53**, 227 (1992).
[5] J. Zhang, S. Huang, and J. Yu, Opt. Lett. **17**, 149 (1992).
[6] R. Jaaniso and H. Bill, Europhys. Lett. **16**, 549 (1991).
[7] A. Kurita and T. Kushida, Opt. Lett. **19**, 314 (1994).
[8] K. Hirao, S. Todorori, D. H. Cho, and N. Soga, Opt. Lett. **18**, 1586 (1993).
[9] M. Nogami, Y. Abe, K. Hirao, and D. H. Cho, Appl. Phys. Lett. **66**, 2952 (1995).
[10] K. Fujita, K. Hirao, and N. Soga, Opt. Lett. **23**, 543 (1998).
[11] M. Nogami, N. Umehara, and T. Hayakawa, Phys. Rev. B **58**, 6166 (1998).
[12] M. Nogami and Y. Abe, Phys. Rev. B **56**, 182 (1997).
[13] M. Nogami and Y. Abe, Appl. Phys. Lett. **64**, 1227 (1994).
[14] M. Nogami and Y. Abe, J. Appl. Phys. **80**, 409 (1996).
[15] H. Song, J. Zhang, D. Gao, S. Huang, and J. Yu, Opt. Commun. **120**, 264 (1995).
[16] T. Schmidt, R. M. Macfarlane, and S. Vöker, Phys. Rev. B **50**, 15 707 (1994).
[17] C. Brecher and L. Ariseberg, Phys. Rev. B **13**, 81 (1976).
[18] D. H. Cho, K. Hirao, and N. Soga, J. Non-Cryst. Solids **189**, 181 (1995).
[19] M. Nogami and T. Hayakawa, Phys. Rev. B **56**, 235 (1997).
[20] M. Nogami, T. Hiraga, and T. Hayakawa, J. Non-Cryst. Solids **241**, 98 (1998).
[21] H. Song, J. Zhang, S. Huang, and J. Yu, J. Lumin. **64**, 189 (1995).